

# Effect of UV Aging on the Tensile and Fracture Mechanical Response of Syndiotactic Polypropylenes of Various Crystallinity

T. Bárány,<sup>1</sup> E. Földes,<sup>2</sup> T. Czigány,<sup>1</sup> J. Karger-Kocsis<sup>3</sup>

<sup>1</sup>Department of Polymer Engineering and Textile Technology, Faculty of Mechanical Engineering, Budapest University of Technology and Economics, H-1111 Budapest, Muegyetem rkp. 3., Hungary

<sup>2</sup>Department of Polymer Physics and Chemistry, Institute of Chemistry, Chemical Research Center, Hungarian Academy of Sciences, H-1525 Budapest, P.O. Box 17, Hungary

<sup>3</sup>Institut für Verbundwerkstoffe GmbH, Universität Kaiserslautern, Pf. 3049, D-67653, Kaiserslautern, Germany

Received 12 February 2003; accepted 8 March 2003

**ABSTRACT:** Syndiotactic polypropylene (sPP) sheets of various crystallinities were subjected to accelerated ultraviolet (UV) aging. The chemical modification of the polymer was followed by FTIR spectroscopy measuring the carbonyl index in transmittance (film) and diffuse reflectance (powder) modes. Both the tensile stress and strain, suitable indicators of the UV aging, changed linearly with the carbonyl index in semilogarithmic representation. The essential work of fracture (EWF) method proved to be less suitable for characterization, as the UV irradiation resulted in surface

embrittlement of the polymer. This caused brittle fracture of the notched specimens instead of the required ductile one. On the other hand, the term of the specific work of fracture related to yielding may adequately reflect the structural and morphological changes of sPP caused by UV irradiation. © 2004 Wiley Periodicals, Inc. *J Appl Polym Sci* 91: 3462–3469, 2004

**Key words:** degradation; fracture; FT-IR; syndiotactic poly(propylene); UV radiation

## INTRODUCTION

Polypropylene (PP) is very sensitive to ultraviolet (UV) degradation, which strongly hampers its outdoor application. The studies of the UV aging of PPs focus mainly on two objects: (a) to find more and more efficient photo stabilizers, and (b) to predict the long-term behavior (durability). The mechanism of photooxidation of PP is well understood, and very effective photostabilizers have been developed on the basis of this knowledge.<sup>1–4</sup> A greathallenge is, however, the assessment of the effects of UV irradiation on the properties, and even more important is to find correlation between indoor (artificial, accelerated) and outdoor weathering.<sup>5,6</sup> It was established that the deterioration of the tensile mechanical properties is a suitable indicator of UV aging. It is still of intensive dispute, whether stress or strain data reflect the UV aging more properly. Attention should be paid to the fact that the residual mechanical properties strongly depend on the preparation of the specimen (type and

conditions of moulding) via severe changes in the supermolecular structure.<sup>5–7</sup> The fracture mechanics may be a suitable alternative to the standardized tensile (static or dynamic) tests. Note that the fracture mechanics yield an inherent toughness value, which is independent of the configuration of the specimen. According to the authors' knowledge, this approach has not been adopted to study the susceptibility of polyolefins to UV irradiation. Therefore, the aim of this work was the determination of the plane stress fracture toughness of two syndiotactic PPs (sPP) of different crystallinity as a function of accelerated UV aging. The toughness was assessed by the essential work of fracture (EWF) concept that belongs to the postyield fracture mechanics. The working hypothesis was that there is a correlation between the oxidation of the polymer (e.g., carbonyl index) and the EWF characteristics. A further aim of this study was: checking the improvement in resistance to UV aging as an effect of enhanced crystallinity. The selection of sPP as a model material was reasoned by the fact that it is sensitive to UV irradiation (although by a lesser extent than isotactic PP<sup>8</sup>) and meets the requirements of the EWF approach at the same time.<sup>9</sup>

## EXPERIMENTAL

### Materials and sample preparation

Two experimental sPP grades of Atofina (Belgium) were involved in this study. Their average molecular

Correspondence to: T. Czigány (czigany#eik.bme.hu).  
collaboration grant between Germany (DAAD) and Hungary (MÖB).

Contract grant sponsor: the National Scientific Research Fund of Hungary; contract grant numbers: T 037687 and T 037864.

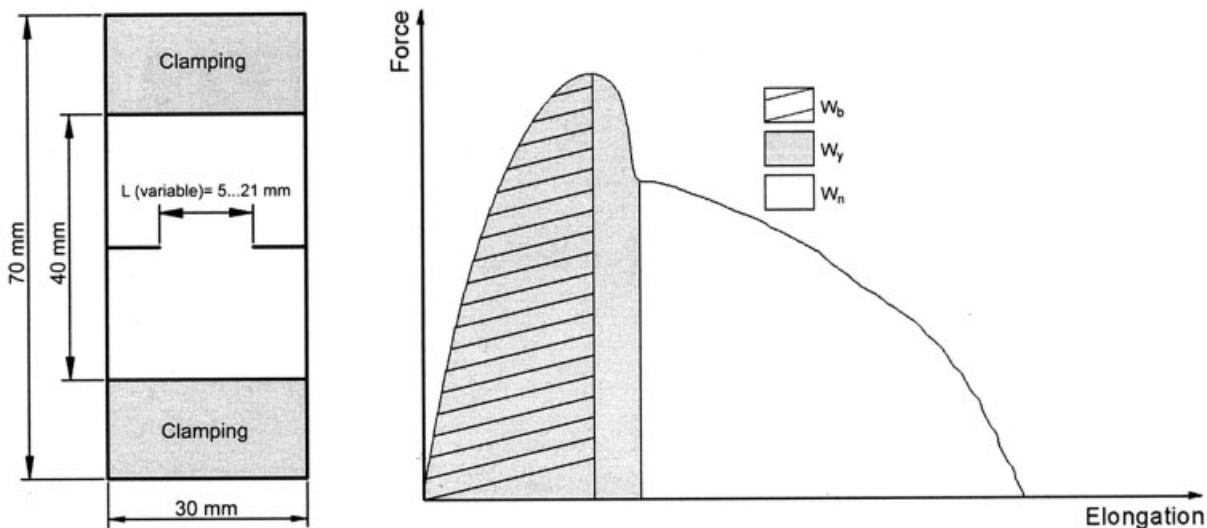


**Figure 1** Dimension of the DDEN-T specimen and a characteristic force vs elongation curve showing the energy partitioning.

masses were comparable; however, they differed in the stereoregularity and thus in crystallinity. The crystallinity of sPP-1 and sPP-2 was about 14 and 18%,

respectively.<sup>9,10</sup> These values were derived by differential scanning calorimetry (DSC), using 207 J/g for the fully crystalline sPP;<sup>11</sup> 0.5 mm thick sheets were

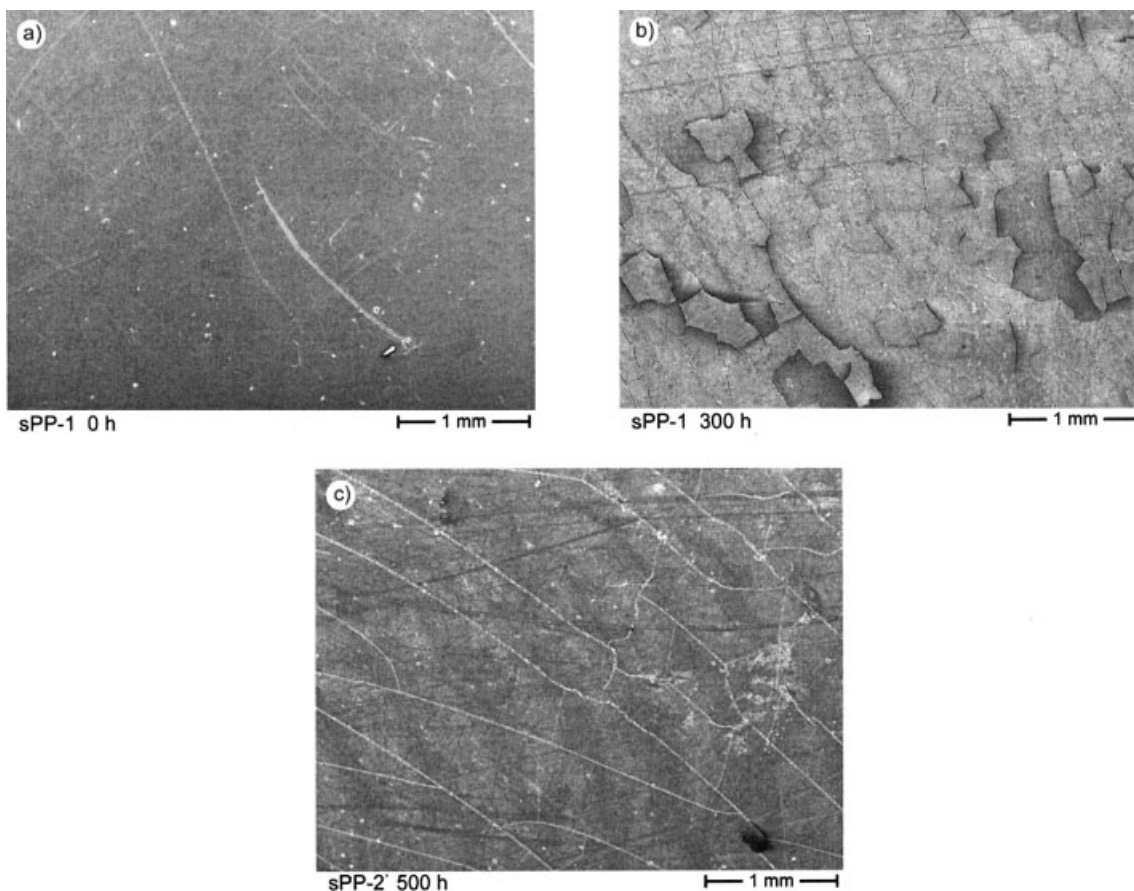


**Figure 2** SEM pictures taken from the surface of (a) sPP-1 prior to UV aging; (b) sPP-1 after 300 h UV aging; (c) sPP-2 after 500 h UV aging.

produced by hot pressing in a Collin (France) press. The pressing conditions were: melting was at 170°C for 10 min and holding at 80°C for 15 min before cooling to room temperature.

### UV aging and its assessment

Rectangular specimens (length: 140 mm, width: 45 mm) cut from the pressed sheets were subjected to UV irradiation from both sides in a Xenotest Alpha LM R138 device (Heraeus, Germany). UV aging was performed up to 500 h. Based on the power of the xenon discharge lamp and the calibrated wavelength range (300–400 nm) the mean irradiation dose was about 27 MJ/m<sup>2</sup> for 100 h (i.e., 13.5 MJ/(m<sup>2</sup> × 100 h) on each side of the specimen).

As the UV irradiation can be followed well by Fourier transform infrared spectroscopy (FTIR) based on the change in the carbonyl band formed,<sup>1–6</sup> this technique was used to trace the aging. Owing to the irradiation-induced surface roughening of the polymer sheets the attenuated total reflection (ATR) method was found less suitable. Therefore, thin sheets (ca. 100 μm) were pressed from the unaged and irradiated material, then scanned in transmission mode in a Mattson-Galaxy 3020 FTIR bench. Five parallel experiments were run for each sample using 16 scans and a resolution of 2 cm<sup>-1</sup>. In addition, diffuse reflectance FTIR (DRIFT) spectra were also taken from the sPP samples ground in liquid nitrogen. In that case the number of scans was 128.

### EFW theory and mechanical tests

EFW postulates a difference between the essential work required for fracture the polymer in its process zone ( $W_e$ ) and the plastic work consumed by various deformation mechanisms in the plastic zone ( $W_p$ ). The total work of fracture ( $W_f$ ) is composed of the two above terms. As  $W_e$  is surface-related, whereas  $W_p$  is volume-related,  $W_f$  can be given by the corresponding specific work terms (i.e.,  $w_e$  and  $w_p$ , respectively):

$$W_f = W_e + W_p = w_e L t + \beta w_p L^2 t \quad (1)$$

$$w_f = \frac{W_f}{L t} = w_e + \beta w_p L \quad (2)$$

where  $L$  is the ligament length,  $t$  is the thickness of the specimen, and  $\beta$  is a shape factor related to the form of the plastic zone.<sup>12,13</sup> The EFW method is widely used to determine the toughness of ductile polymers, including isotactic<sup>14</sup> and syndiotactic<sup>9</sup> PPs, especially in film and sheet forms.

The EFW terms were determined by using double, deeply edge-notched tensile (DDEN-T) specimens of

the following dimensions: overall length: 70 mm, width 30 mm, ligament length ( $L$ ): varied between 5 and 21 mm (Fig. 1). The DDEN-T specimens were notched by pressing a jig containing two razor blades of variable distance. At every ligament length four specimens were tested at a deformation rate of 1 mm/min. Figure 1 depicts the DDEN-T and a characteristic force vs elongation curve where the energy partitioning is indicated. The following basic equation was used for the data reduction (Fig. 1):

$$w_f = w_e + \beta w_p L = w_{e,y} + w_{e,n} + \beta' w_{p,y} L + \beta'' w_{p,n} L \quad (3)$$

where subscriptions  $y$  and  $n$  correspond to yielding and necking, respectively.

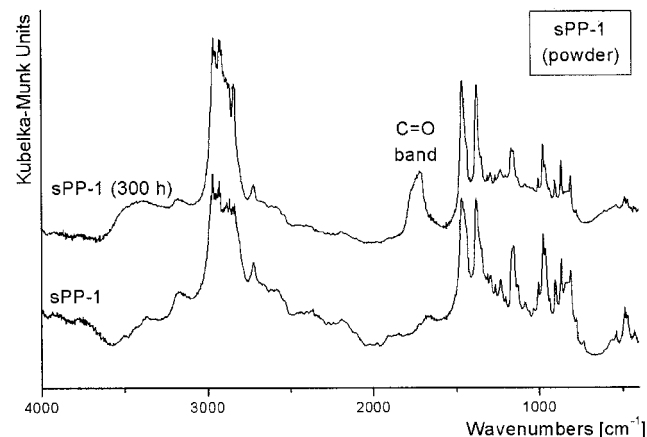
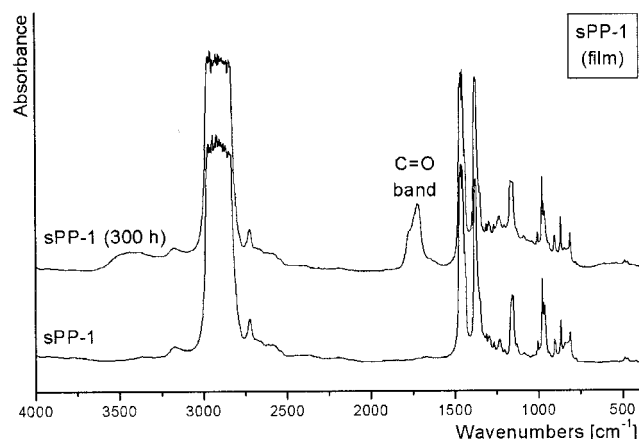


**Figure 3** FTIR spectra of sPP-1 before and after UV aging for 300 h. (a) Measured in transmittance on films compression molded from sheets; (b) measured by DRIFT on powder samples ground from sheets.

**TABLE I**  
Dependence of the Carbonyl Index on the Type of sPP, the Time of UV Aging, and the Measuring Technique

Sample	UV-aging (h)	Carbonyl index	
		Film	Powder
sPP-1	0	0.127	0.454
	100	1.029	2.385
	200	2.663	5.194
	300	5.592	7.416
sPP-2	0	0.140	0.599
	200	0.172	0.627
	300	0.347	1.15
	500	1.449	2.837

Note that the EWF terms related to the crack tip blunting process were also assessed (cf. Fig. 1).

Tensile tests were performed on dumbbells (EN ISO 527, type: 1B) at a deformation rate of 1 mm/min. The elastic modulus ( $E$ ), the yield strength ( $\sigma$ ), and the yield strain ( $\epsilon$ ) were deduced. Note that no yielding occurred after aging, and thus  $\sigma$  and  $\epsilon$  represent the related ultimate values.

### Fractography

The failure mode of DDEN-T specimens was studied in a scanning electron microscope (SEM; JEOL JSM 5400, Japan) after sputtering the fracture surface with gold. The UV-induced surface cracking of the sPP sheets was also inspected by SEM.

## RESULTS AND DISCUSSIONS

### FTIR response

As was described above, the chemical modification of the polymer could not be followed by FTIR-ATR tech-

nique due to roughening of the surface caused by the UV-irradiation. The surface pattern resembling a dried soil after aging is shown in Figure 2. One can clearly recognize that the density of the surface fissure is considerably higher in the less crystalline sPP-1 than in the more crystalline sPP-2 irradiated for a longer time. This is the first hint that the more crystalline sPP-2 has higher stability against UV-aging than the less crystalline sPP-1.

Figure 3 displays the FTIR spectra of sPP-1 before and after UV aging for 300 h. In the latter case, the carbonyl absorption band became obvious. Recall that the carbonyl band is considered the most suitable indicator for UV aging in polyolefins.

The carbonyl index values of the film samples [Fig. 3(a)] were determined by relating the integral absorption of the C=O group [T(1850–1563)] to that of the double absorption band of sPP between 998 and 940  $\text{cm}^{-1}$  [T(998–940)]. This band was selected as internal standard because the bands of  $\text{CH}_2$  at 1510–1410  $\text{cm}^{-1}$  and  $\text{CH}_3$  at 1410–1320  $\text{cm}^{-1}$  have too high intensities. Therefore, they could not be used for quantitative evaluation. The absorption at 998–940  $\text{cm}^{-1}$  is less intense, and T(998–940) changes linearly with the samples thickness, independent of the history of the material. The carbonyl index values calculated are given in Table I. The nonirradiated polymer itself has some small absorption at 1800–1600  $\text{cm}^{-1}$ , which can be attributed to the effect of oxidation during processing. The same internal standardization was used for the DRIFT spectra [Fig. 3(b)], and the carbonyl index values are listed also in Table I (“powder”). There is good correlation between the carbonyl indices, measured in the transmittance mode (absorbance values), and by DRIFT (Kubelka-Munk units), although the relationship is not linear. Linear correlation can be obtained by plotting the carbonyl indices in double

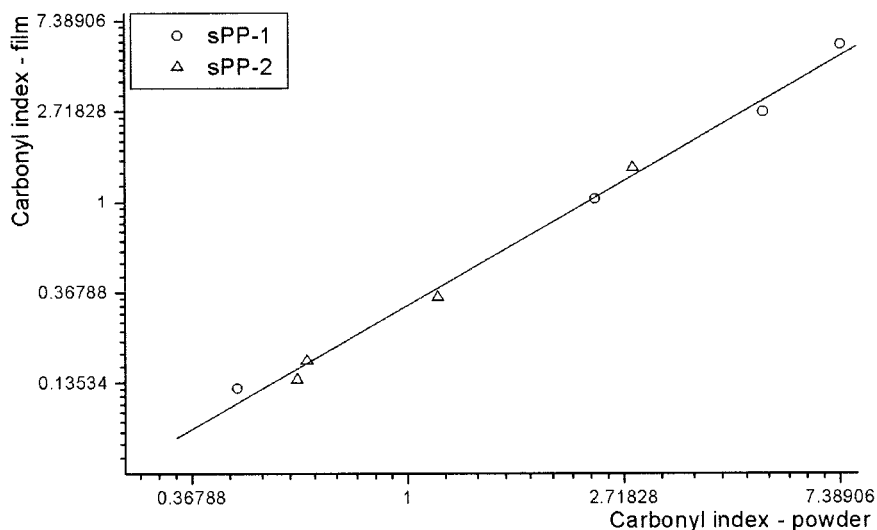


**Figure 4** Relationship between the carbonyl index values deduced from DRIFT (powder) and absorbance (film) spectra.



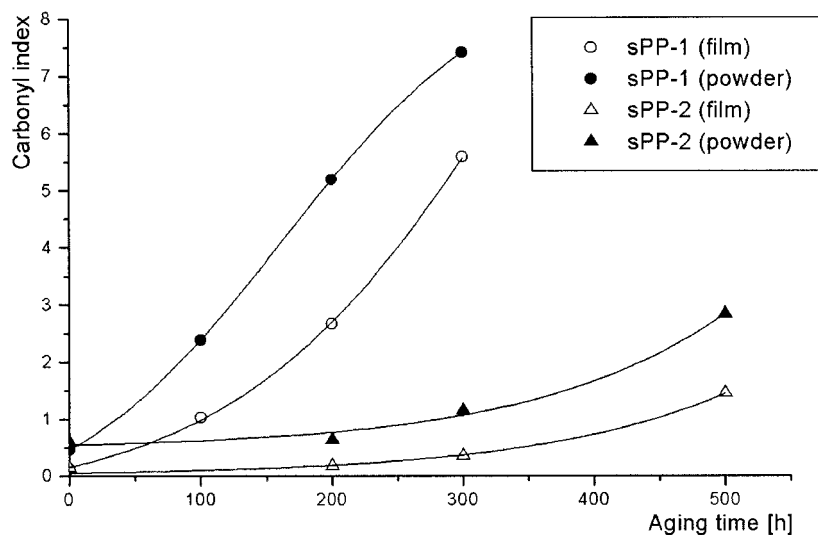


Figure 5 Changes of the carbonyl index values with aging time.

logarithmic scale, as can be seen from Figure 4. Figure 5 shows the carbonyl index development with UV aging for both sPPs studied. Figure 5 clearly demonstrates that the less crystalline sPP-1 is markedly more sensitive to UV-aging than the more crystalline sPP-2. This finding is in harmony with expectation.

### Tensile mechanical behavior

Table II lists the  $E$ -modulus ( $E$ ), the yield strength ( $\sigma$ ), and the yield strain ( $\varepsilon$ ) values for the two sPPs as a function of UV aging. Note that brittle fracture took place instead of yielding after irradiation, and thus the related values represent ultimate ones. One can notice that higher crystallinity is associated with higher stiffness ( $E$ ) and strength. On the other hand,  $\varepsilon$  seems to be less sensitive to crystallinity. The UV aging resulted in a strong decrease of  $\sigma$  and  $\varepsilon$  but in an increase of  $E$ . Linear correlation was obtained by plotting  $\sigma$  and  $\varepsilon$  as a function of the carbonyl index in semilogarithmic scales (Fig. 6). The beauty of this correlation is that the full embrittlement of sPP can be assigned to a threshold carbonyl index (interception of the related curves with the x-axis). On the other hand, no unequivocal correlation could be found between  $E$  and the carbonyl index. The above finding clearly supports that the presently used tracing of UV aging via changes in the static tensile properties (i.e.,  $\sigma$ ,  $\varepsilon$ ) is correct. It is worth noting that the scatter in the  $E$  modulus becomes quite large with advanced aging even when an incremental extensometer is used.

### EFW response

The EWF method proved to be adequate for the characterization of unaged sPPs. As can be seen from

Figure 1, blunting ( $w_b$ ), yielding ( $w_y$ ), and necking ( $w_n$ ) could be easily separated. Furthermore, the shape of the force vs elongation curves was "self-similar," which is the major criterion of the EWF application. Higher crystallinity of sPP was reflected in an increase of the essential work of fracture related to yielding ( $w_{e,y}$ ). The UV aging caused severe embrittlement, as shown already by the tensile mechanical results. This was also observed in the force vs elongation curves monitored on the DDEN-T specimens (Fig. 7). With increasing time of aging the necking stage disappeared first. This was followed by limitations in yielding and blunting, then ended in fully brittle fracture. Recall that the EWF method is not valid for brittle fracture. Therefore, the traditional tensile mechanical tests are more adequate for following the UV degradation. The EWF parameters determined are listed in Table III. These results prove that the UV aging is less well characterized by EWF than by tensile testing (Table II) because of the early onset of brittle fracture.

TABLE II  
Static Tensile Characteristics of sPPs of Various Crystallinity as a Function of UV Aging

Sample	UV-aging (h)	Static tensile characteristics		
		E modulus (MPa)	$\sigma$ (MPa)	$\varepsilon$ (%)
sPP-1	0	568	15.1	4.8
	100	621	8.9	1.6
	200	635	4.9	0.9
	300	655	1.5	0.4
sPP-2	0	599	18.1	4.6
	200	630	17.2	4.4
	300	660	16.0	3.9
	500	685	6.5	1.8

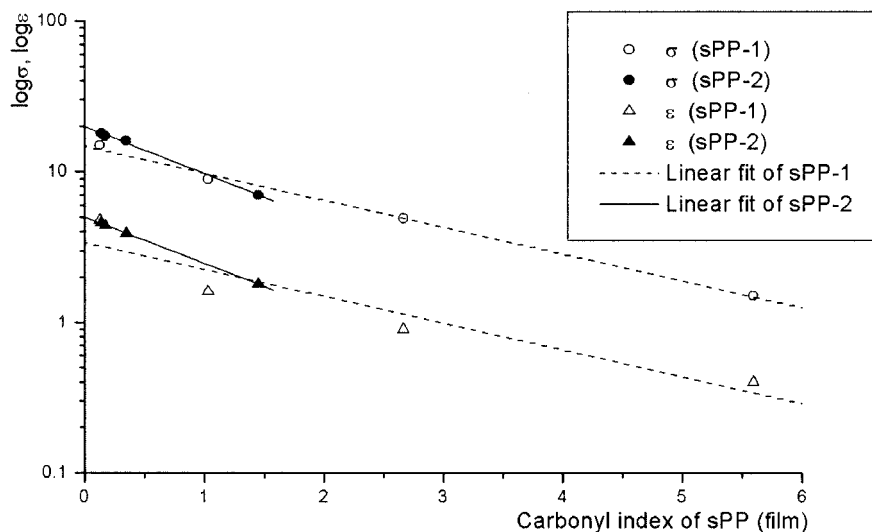


**Figure 6** Changes in the yield stress ( $\sigma$ ) and strain ( $\epsilon$ ) of sPPs as a function of carbonyl index determined from transmittance spectra.

It was shown that the most reliable EWF term is  $w_{e,y}$  as it can be considered an inherent toughness parameter (representing plane strain type fracture).<sup>12,15</sup>  $w_{e,y}$  (and also the term related to blunting,  $w_{e,b}$ ) decreases with increasing UV aging time in the case of sPP-1. It goes through a maximum for sPP-2, which is quite unexpected, as the tensile stress and strain values decreased monotonically with aging (Table II). This “reinforcing effect” can be attributed to some post-crystallization of sPP-2 under the UV conditions. The scission of the polymer chains caused by UV irradiation may result in some post crystallization of sPP above the glass transition temperature ( $T_g$ ). Recently, the recrystallization of isotactic PP was proved under

such conditions.<sup>16</sup> This process is responsible for the increase in toughness. At the same time the number of tie molecules decreases (due to the processes chain breaking and post crystallization), which leads to toughness reduction and to brittle fracture. This mechanism proposed recently<sup>17</sup> has to be checked for the present systems.

**Failure mode**

The change in the failure behavior is demonstrated in Figure 8 on the example of sPP-2. Figure 8(a) shows that the unaged sPP-2 failed by ductile tearing. The undulation in the fractured specimen is characteristic

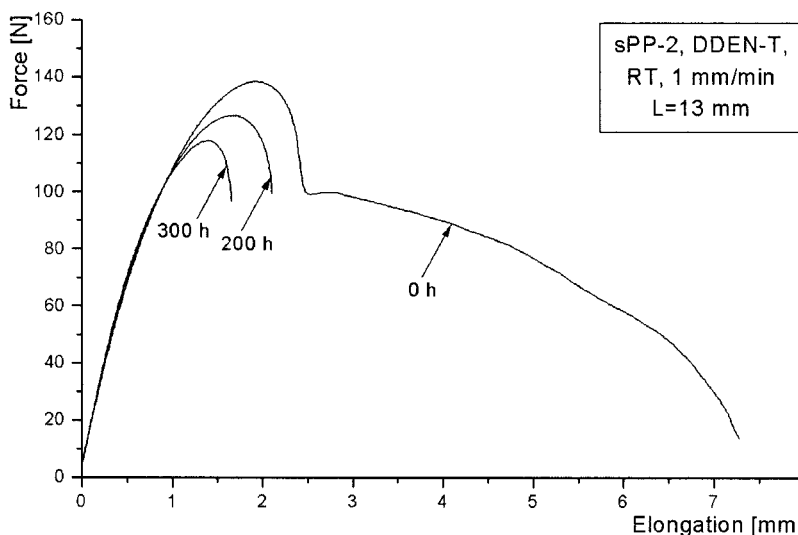


**Figure 7** Changes in the force vs elongation curves of DDEN-T specimens of sPP-2 at constant ligament length as an effect of UV aging.

**TABLE III**  
Parameters of the Work of Fracture of sPPs as a Function of UV Aging

Sample	UV-aging (h)	Essential work of fracture (kJ/m <sup>2</sup> )			Nonessential work of fracture (MJ/m <sup>3</sup> )
		$w_e$	$w_{e,y}$	$w_{e,b}$	$\beta w_p$
sPP-1	0	27.1	4.1	3.6	3.7
	100		brittle		brittle
sPP-2	0	29.9	5.7	4.5	3.6
	200	—	10.4	7.2	—
	300	—	8.5	6.7	—
	500		brittle		brittle

The correlation coefficients of the linear regressions (eqs. 1 and 3) were >0.96 except for sPP-2 aged for 300 h (0.71).

for thermoplastic rubbers<sup>18</sup> where sPP also belongs.<sup>19</sup> The driving force of the undulation pattern is the resilience of the material. Because of that, the initial fracture path becomes smaller and thus undulated.

The fracture surface of sPP-2 became brittle after 300 h UV aging except for the central zone, which showed ductile tearing [Fig. 8(b)]. The flat fracture surface already indicates the transition from plane stress to plane strain condition. The plane strain

toughness is believed to be represented by  $w_{e,y}$ . The high magnification SEM picture [Fig. 8(c)] demonstrates the surface embrittlement caused by UV aging. One can also recognize that the depth of the surface cracks shown in Figure 2 agrees fairly well with that of the embrittled surface layer (arrows indicate). Figure 8(b) and (c) also highlights the basic difference between the tensile and fracture mechanical responses. Residual tensile strength and strain values can be de-

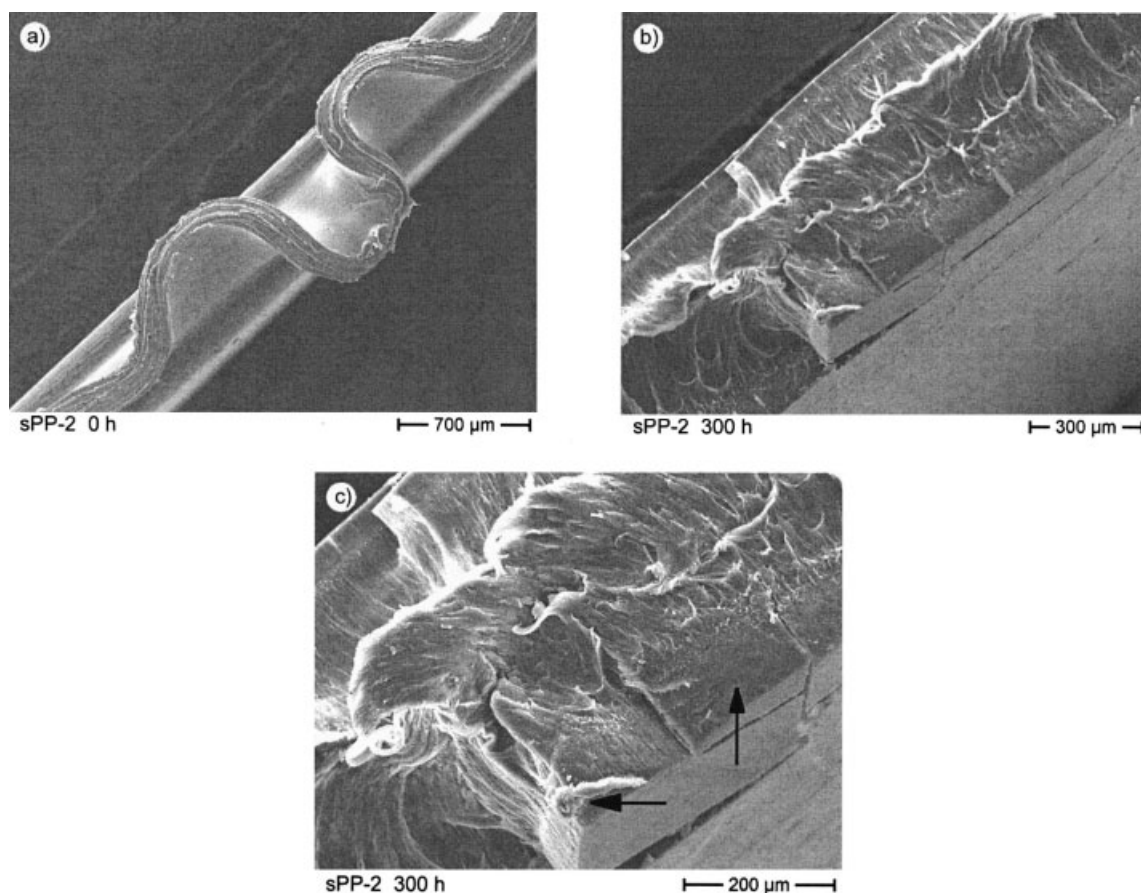


**Figure 8** SEM pictures taken from the fracture surface of DDEN-T specimens of sPP-2 tested before (a) and after 300 h UV aging (b,c).

terminated on specimens that fail in mixed (brittle/ductile) manner. On the other hand, the occurrence of mixed failure limits the applicability of EWF. It should be mentioned here that an attempt was made earlier to use the EWF method for specimens that failed in brittle/ductile manner.<sup>20</sup> This approach could also be adopted in this case, as the surface parts broken brittlely and ductilely can be well distinguished from one another.

### CONCLUSIONS

In this work the aging of syndiotactic polypropylenes (sPP) of various crystallinity caused by ultraviolet (UV) irradiation was studied by different methods. The chemical modification was followed by infrared spectroscopy. The mechanical properties were characterized by tensile tests and the essential work of fracture (EWF) method. From the results the following conclusions were drawn:

1. The progress of the UV aging is well reflected in the change of the carbonyl index determined by FTIR spectroscopy either in film (transmission) or in powder (DRIFT).
2. The tensile strength and strain values are good indicators of the UV aging. Both of them changed linearly with the carbonyl index when plotted in semilogarithmic scales.
3. The EWF parameters, even the ones related to yielding, are less suitable than the tensile characteristics, as the specimens embrittle on their surface and fracture in a mixed manner (brittle/ductile) after aging. Therefore the applicability of the EWF approach is limited. On the other hand, changes in the specific essential work of fracture

related to yielding may deliver useful information on the molecular and morphological alterations caused by aging.

### References

1. Rabek, F. R. *Polymer Photodegradation, Mechanism and Experimental Methods*; Chapman & Hall: London, 1995, p. 84, vol. 3.
2. Tüdös, F.; Bálint, G.; Kelen, T. In *Developments in Polymer Stabilization-6*; Scott, G., Ed.; Applied Science Publishers Ltd: Barking, England, 1983, p. 121, vol. 4.
3. Al-Malaika, S. In *Polypropylene: An A-Z Reference*; Karger-Kocsis, J., Ed.; Kluwer Academic Publishers: Dordrecht, 1999, p. 581.
4. Gugumus, S. *Polym Degrad Stabil* 1993, 39, 117.
5. White, J. R. In *Polypropylene: An A-Z Reference*; Karger-Kocsis, J., Ed.; Kluwer Academic Publishers: Dordrecht, 1999, p. 866.
6. White, J. R.; Turnbull, A. *J Mater Sci* 1994, 29, 584.
7. Ogier, L.; Rabello, M. S.; White, J. R. *J Mater Sci* 1995, 30, 2364.
8. Kato, M.; Tsutura, A.; Kuroda, S.; Osawa, Z. *Polym Degrad Stabil* 2000, 67, 1.
9. Karger-Kocsis, J.; Bárány, T. *Polym Eng Sci* 2002, 42, 1410.
10. Karger-Kocsis, J.; Shang, P. P. *J Therm Anal Calorim* 2002, 69, 499.
11. Supaphol, P. *J Appl Polym Sci* 2001, 79, 1603.
12. Karger-Kocsis, J. In *Fracture of Polymers, Composites and Adhesives*; Williams, J. G.; Pavan, A., Eds.; Elsevier Science: Oxford, 2000, p. 213, vol. 27.
13. Mai, Y.-W.; Wong, S.-C.; Chen, X.-H. In *Polymer Blends Formulations and Performance*; Paul, D. R.; Bucknall, C. B., Eds.; Wiley: New York, 1999, p. 17, vol. 2.
14. Ferrer-Balas, D.; Maspocho, M. L.; Martinez, A. B.; Ching, E.; Li, R. K. Y.; Mai, Y.-W. *Polymer* 2001, 42, 2665.
15. Karger-Kocsis, J.; Ferrer-Balas, D. *Polym Bull* 2001, 46, 507.
16. Ddic, D.; Kostoski, D.; Djokovic, V.; Stojanovic, Z. *Polym Degrad Stab* 2000, 67, 233.
17. Karger-Kocsis, J. I *Structure Development during Polymer Processing*; Cunha, A. M.; Fakirov, S., Eds.; Kluwer Academic Publishers, Dordrecht, 2000, p. 163.
18. Mouzakis, D. E.; Gahleitner, M.; Karger-Kocsis, J. *J Appl Polym Sci* 1998, 70, 873.
19. Loos, J.; Schimanski, T. *Polym Eng Sci* 2000, 40, 567.
20. Mouzakis, D.E.; Karger-Kocsis, J. *Polym Bull* 1999, 42, 473.